A numerical method to integrate duration-of-load and bacterial deterioration for long-standing timber piles

Yang, Changxi; Khaloian-Sarnaghi, Ani; Yu, Taoyi; van de Kuilen, Jan Willem

DOI
10.1007/s00226-025-01652-8

Publication date
2025

Document Version
Final published version

Published in
Wood Science and Technology

Wood Science and Technology (2025) 59:46
https://doi.org/10.1007/s00226-025-01652-8

ORIGINAL

A numerical method to integrate duration-of-load and bacterial deterioration for long-standing timber piles

Changxi Yang[1] · Ani Khaloian-Sarnaghi[1] · Taoyi Yu[1] · Jan-Willem van de Kuilen[1,2]

Received: 13 August 2024 / Accepted: 24 March 2025 / Published online: 10 April 2025

Abstract
The strength degradation resulting from duration-of-load (DOL) effect and bacterial decay poses significant challenges to historical timber piles. Many historical European cities still heavily rely on the infrastructure supported by their original timber foundations. A reliable modelling approach on the structural performance of timber piles is needed to avoid the economic loss caused by closing down infrastructure. In this work, we consider a simplified bacterial decay model and develop a numerical framework to integrate the decay model into a standard DOL model. Two approaches are proposed and compared: one considering the homogenised effect of bacterial decay over the entire cross section, and the other taking into account the localised failure accelerated by bacterial decay and applying stiffness reduction to allow stress redistribution. Although the homogenised failure criterion is found to potentially underestimate the effect of bacterial decay, both approaches are able to capture the designated decay pattern. Ultimately, there is a potential for future extension to more intricate loading conditions and decay patterns.

Introduction

Before the widespread usage of steel and concrete in the 20th century, timber piles were frequently employed in soft-ground foundations to reach deeper soil layers (Przewłócki et al. 2005; Klaassen 2008; Zelada-Tumialan et al. 2013). Even today, timber piles remain widely used in road and railway infrastructure in the US, Canada,

✉ Changxi Yang
changxi.yang@tum.de

[1] TUM School of Engineering and Design, Department of Materials Engineering, Professorship of Wood Technology, Technical University of Munich, Winzererstraße 45, 80797 Munich, Germany

[2] Chair of Biobased Structures and Materials, Delft University of Technology, Postbus 5, Delft 2600 AA, The Netherlands

Australia, Sweden and the Netherlands (Gunnvard et al. 2021). Many historical European cities such as Amsterdam, Venice, Stockholm and Ljubljana, are still supported by their original timber piles. During the last decades, severe wood degradation has been discovered on a considerable number of foundations across Europe (Ceccato et al. 2013; van de Kuilen et al. 2022; Humar et al. 2021), partially leading to structural failure. To prevent such structure failure and maintain the safety of foundations, deteriorated timber piles need to be identified, either repaired or replaced. However, these interventions often come with significant financial burdens, sometimes accounting for up to half of the total renovation costs (Klaassen 2008). Notably, Zelada-Tumialan et al. (2014) reported that the typical cost of underpinning pile foundations for a row house ranges between $200,000 and $250,000 in Boston. Given the significant demand and economical costs for inspection and repair, a clear need is posed there for an effective assessment method.

To create a near anaerobic condition, timber piles are generally placed below the lowest expected groundwater level (Przewłócki et al. 2005; Klaassen 2008; Elam and Björdal 2020). For these waterlogged environments, biological decay mainly originates from bacteria. Only in cases where the dissolved oxygen in groundwater reaches a certain threshold, soft rot fungi decay may take place (Zelada-Tumialan et al. 2014). Bacterial decay rate is generally low and the service life of timber piles in submerged water can be up to 500 years (van de Kuilen et al. 2022). However, several factors can accelerate the deterioration process and shorten the service life. For instance, water pumping, mining cavities, or urban underground constructions can lead to a decrease

in groundwater level. With the increased oxygen level in the soil, a more favourable condition is created for aggressive fungal degradation (Elam and Björdal 2020; Przewłócki et al. 2005). Climate change may be another factor, as increased soil temperature is known to promote bacterial activities (Díaz-Raviña et al. 1994). Moreover, many historical foundations face challenges due to changes in loading conditions (Przewłócki et al. 2005). This can lead to nonuniform settlement and increased stress on certain parts of the foundation, accelerating damage accumulation caused by long-term mechanical loading. Due to the abovementioned effects, the actual service life of historical timber piles can be largely reduced. For instance, Zelada-Tumialan et al. (2014) estimated that the service life might be shortened to around 100 years, based on historical pile data from downtown Boston.

The ‘duration of load’ (DOL) effect describes the dependency of material strength on both the magnitude and the duration of loads (Svensson 2009). Even at a stress level significantly lower than the short-term strength, microscopic cracks may develop in wood. Propagation of these cracks under long-term sustained loading may eventually lead to macroscopic failure of the component or the structure. In general, research on DOL effect falls into three categories: phenomenological models (Wood 1951), models based on fracture mechanics (Nielsen 1979) and models based on chemical kinetics (Caulfield 1985; van der Put 1989). The latter two categories, despite the capability of incorporating physical mechanisms, are rather intricate for engineering uses. In contrast, phenomenological models are simple in form and have been validated through extensive experimental studies (van de Kuilen and Gard 2012). By introducing a damage accumulation coefficient α that develops over time, the extent of ‘damage’ can be measured, facilitating the prediction of time to failure for specific material-load combinations.

Two types of bacteria are distinguished, which can degrade wood: the tunnelling bacteria and the erosion bacteria. The former accesses all areas of wood cell walls and requires the presence of oxygen, whereas the latter survives very low oxygen levels or even in anoxic conditions, creating troughs into wood fibre cell walls and weakening the strength of wood (Sundararaj 2022). Erosion bacteria degrade mostly the cellulose-rich S2 layer, whereas the middle lamella and S3 layer remain intact (Klaassen 2008). Therefore, on-site inspections may not distinguish degraded wood from sound wood based on the appearance. However, the degraded wood could be much softer and even spongy, depending on the extent of degradation. Studies conducted at various sites have confirmed that erosion bacteria are the primary biological agents responsible for the degradation of waterlogged wooden piles (Boutelje and Bravery 1968; Boutelje and Göransson 1975; Grinda 1997; Klaassen 2008; Rehbein et al. 2013; Elam and Björdal 2020). It has also been shown that wood already degraded by bacteria can become vulnerable to aggressive fungal attacks if microclimate or groundwater changes occur (Gjelstrup Björdal 2012; Elam and Björdal 2020).

Gard et al. (2024) and Mirra et al. (2024) conducted an extensive experimental investigation on timber piles extracted from foundations aging 100 to 300 years in the city of Amsterdam. Following observations were made:

- Decay pattern: bacterial decay generally appeared close to the periphery on a cross section, whereas no bacterial decay was detected in the inner heartwood area. This is consistent with previous findings that heartwood, generally rich in extractives, is less susceptible to bacterial decay (Zelada-Tumialan et al. 2013; Elam and Björdal 2020; Mirra et al. 2024);
- Strength reduction due to various degradation mechanisms: for specimens taken from the same year, compressive strength reduction in severely decayed specimens was up to half that of sound specimens; for specimens with 200-year age difference, sound wood in the inner area also experienced strength reduction due to the DOL effect, which could be up to 30%.
- Remaining load carrying capacity of timber piles: compressive tests conducted on full-scale pile sections showed a negative correlation between remaining strength and decay depth.

Current design codes do not provide guidance on assessment of the remaining service life of historical timber piles. The DOL effect is simply considered in the design stage through a discrete strength modification factor. Whereas biological degradation is only evaluated qualitatively, by assigning a durability and a hazard class to specific combination of material and environmental conditions. As stated by Gard et al. (2024), the current method often leads to over-conservative design, which is economically costly and unnecessary.

Based on the exponential damage accumulation function developed by Gerhards (1987), van de Kuilen and Gard (2012) proposed a modified damage function that includes the effect of biological degradations. After the initiation of biological decay, the material strength was substituted with an averaged strength over the cross section. Therefore, they successfully incorporated the decay depth and the decay-induced strength degradation into the damage function, making it an effective approach for engineering practices.

The aim of this paper is to develop a numerical modelling framework for assessing the structural performance of historical timber piles. A simplified pile problem is modelled for the verification of the developed approach, which incorporates two strength degradation mechanisms– DOL effect and bacterial decay. For simplification, the model does not account for accelerated damage resulting from climate or groundwater changes. Two main objectives of this paper are:

- To propose a practical bacterial decay model that can be implemented into FE modelling, on the basis of previous results from retrieved historical timber piles (Pagella and Ravenshorst 2022), where the decay pattern can be identified.
- To integrate the proposed bacterial decay model, developed by van de Kuilen and Gard (2012) into a standard DOL model, which can be used as phenomenological failure criteria for numerical mechanical analysis.

Materials and methods

Materials

The simulation problem considered in this study is based on experimental observations made by Pagella and Ravenshorst (2022). To better demonstrate the influence of bacterial decay on the structural performance, a reference spruce pile dated back to 1727 is selected, which is one of the oldest piles featured by severe decay development.

The extracted pile section is a tree trunk of 11 m length with naturally tapered shape. Because of the narrower cross section at the top of the tree trunk, the pile was inserted into soil upside down. While previous studies suggest that bacterial decay depth remains relatively uniform along the pile length (Klaassen 2008; Zelada-Tumialan et al. 2013), all reference piles in this work exhibited more severe decay at the pile tip, where the cross section is smallest (Pagella and Ravenshorst 2022). Therefore, in this work, the pile tip is assumed to be the governing cross section for uniaxial loading conditions. For the ease of simulation, the tip radius of 75 mm is taken to form a cylindrical geometry. Preliminary study has shown a higher stress level of a model with reduced height. However, running simulations for a full-scale pile is computationally expensive. Considering that the current work focuses on developing a modelling framework rather than to validate full-scale piles, the height of the pile is reduced from 11 m to 200 mm for the conducted simulation in this study.

The material elasticity properties of spruce used in this study are listed in Table 1. For the strength properties, an initial compressive strength value of 14.4 MPa is adopted. The applied longitudinal Modulus of Elasticity (MoE) and strength are obtained by Pagella et al. (2024), using wet-conditioned new piles. The elastic properties in other directions are estimated based on elastic ratios from the Wood Hand-

Table 1 Elastic parameters used in this work, calculated based on laboratory (2021) and Pagella et al. (2024)

E_R	E_T	E_L	μ_{RT}	μ_{RL}	μ_{TL}	G_{RT}	G_{LR}	G_{LT}
686.4	378.4	8800	0.435	0.04	0.025	26.4	563.2	536.8

book (Laboratory 2021). As a simplification, constant Poisson's ratios independent of moisture content are taken.

DOL model and bacterial decay model

A standard exponential damage accumulation equation is selected to model the DOL effect. As shown in Eq. 1, the damage accumulation coefficient α is a latent signal of specimen failure deducted from long-term experiments with certain load history (Gerhards and Link 1987). The value of α starts from zero and increases over time until it reaches one, indicating complete failure of the specimen. Model parameters A and B are estimated as: A=31.2, B=29.6 according to Gerhards and Link (1987).

$$\frac{d\alpha}{dt} = exp\left(-A + B \cdot \frac{\sigma\ (t)}{f_s\,(t)}\right) \tag{1}$$

In Eq. 1, $\frac{d\alpha}{dt}$ is the damage accumulation rate per minute; $A,\ B$ are model constants; $\sigma\ (t)$ is the time-dependent stress; $f_s\,(t)$ is the time-dependent strength.

The bacterial decay depth on the extracted pile section was 15 mm and 40 mm for pile head and pile tip, respectively (Pagella and Ravenshorst 2022). Taking into account that bacterial decay is generally a very slow process (Gard et al. 2024; Sundararaj 2022), the author assumes an onset of bacterial decay after 90 years. By simplifying the decay development to a linear process, a fast decay rate of 0.2 mm/year at the tip and a slow decay rate of 0.07 mm/year at the head are distinguished (Eq. 2). The decay rate model is linearly interpolated to the pile section between tip and head. As an initial attempt, the current work takes into account a uniform sapwood width of 40 mm over the whole length of the pile and consider heartwood as free of bacterial attack, with a decay rate of 0 mm/year. Based on the work by Mirra et al. (2024), the strength reduction caused by bacterial decay is taken as 50% of the initial strength. As an initial approximation, the stiffness is also considered to reduce by 50% due to bacterial decay.undefined

$$\left\{ \begin{array}{c} d = 0,\ \ t \leq\ 90yr \\ d = min(40, (T-90) \times\ 0.2),\ \ t > 90yr\ \ (pile\,tip) \\ d = min(40, (T-90) \times\ 0.07),\ \ t > 90yr\ \ (pile\,head) \end{array} \right. \tag{2}$$

In Eq. 2, d is the decay depth; t is the operation time of the pile in year.

Simulation setup

The pile geometry mentioned in sec. Materials is built in the software ABAQUS/Standard (Simulia 6.14, from Dassault Systems). A cylindrical coordinate system is selected with the pith located at the centre of the cross section. C3D4 elements with a mesh size of 5 mm have been used for simulations, as suggested by the convergence study presented in sec. Convergence study. Real foundation piles may be subjected to a combination of loads and much more complex boundary conditions (compressive load and bending moment at the pile, shear forces along the pile length, uneven lateral forces from soil and/or water, etc.). However, the current work focuses on the development of the numerical framework. In order to be able to verify the developed model analytically at the first step, the loading and boundary conditions have been simplified to a uniaxial load with fixed constraints at the bottom of the sample. Although the model may be simplified to an axisymmetric model, 3D FEM elements are implemented in this work, as real-world observations generally show non-symmetric decay pattern, loading and boundary conditions. As illustrated in Fig. 1, the bottom surface (pile tip) is clamped. A constant load is applied on the top surface (pile head). As a conservative estimate, the load is taken as 30% of the initial load carrying capacity. The material behavior was developed and programmed in UMAT. Due to the relatively low stress level, it is reasonable to assume that the material does not exhibit plastic behavior at the initial state. The potential plasticity developed after decay development is excluded from the current study as a simplification. Therefore, linear orthotropic elasticity is implemented in UMAT.

Numerical algorithm development

In the presence of bacterial decay, the cross section can be divided into a decayed part and a sound part. Assuming that the sound part has the same original mechanical properties as new timber, the reduced mechanical properties at the decayed area

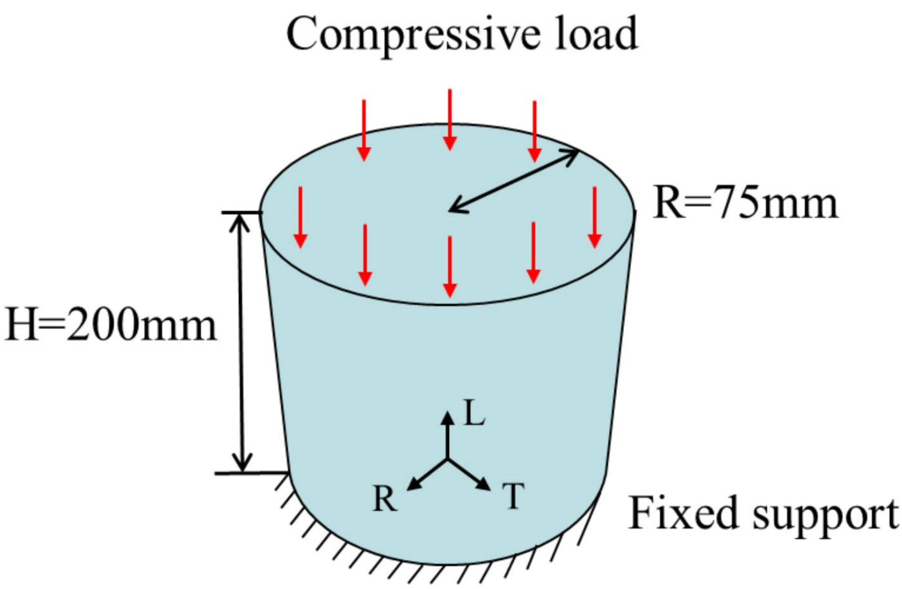

Fig. 1 Illustration of the modelled pile section

result in stress redistributions, increasing the stress level of the remaining part. Since the applied damage accumulation model calculates the damage rate dα/dt merely based on the stress level, the raised stress level accelerates damage accumulation and results in faster failure.

In the following subsections, two distinct approaches are proposed to numerically implement the abovementioned DOL model and bacterial decay model. In both approaches, DOL and bacterial decay are considered as two separate damage processes that interact through the altered stress ratio in the exponential DOL equation. The damage due to DOL is progressive and develops exponentially, determining the final structural failure. The damage caused by bacterial decay is simplified to an abrupt process that leads to 50% stiffness and 50% strength reduction once initiated.

Approach 1– homogenised failure criterion

The analytical modelling approach by van de Kuilen and Gard (2012), represented by Eq. 3, can be directly implemented through a homogenised failure criterion.

$$\frac{d\alpha}{dt} = exp\left(-A + B \cdot \frac{\sigma\ (t)}{f_s\,(t)}\right) = exp\left(-A + B \cdot \frac{F\,(t)}{F_u\,(t)}\right) \tag{3}$$

where, $F\,(t)$ is the time-dependent load on the specimen; $F_u\,(t)$ is the time-dependent load carrying capacity of the specimen, which is influenced by bacterial decay following Eq. 4.

$$F_u\,(t) = (1 - 0.5 \cdot \frac{A_{decay}\,(t)}{A_{tot}}) \cdot f_{s,0} \cdot A_{tot} \tag{4}$$

where, $A_{decay}\,(t)$ and A_{tot} represent the decayed and the total cross-sectional area, respectively. Parameter $f_{s,0}$ indicates the initial strength value of new sound wood.

As depicted in Fig. 2, upon entering each increment, the decay depth is calculated according to the decay model stated in sec. DOL model and bacterial decay model. A field variable indicating decay is assigned to each material point accordingly. Different field variable values influence the stiffness value of the material point, which is further used in deformation calculations carried out by ABAQUS built-in algorithm. A separate damage accumulation coefficient calculation is performed outside the deformation calculation through two user-defined subroutines – USDFLD and URDFIL. The calculated damage accumulation coefficient α is then stored into a state variable as output. Since α is calculated based on the averaged load carrying capacity over the cross-sectional area, an equal value of α for all material points is expected, which demonstrates the homogenised effect of bacterial decay on damage accumulation.

Approach 2 – localised failure criterion

In the second approach, a local damage accumulation coefficient α is calculated for each material point based on the local stress and strength values. A major difference

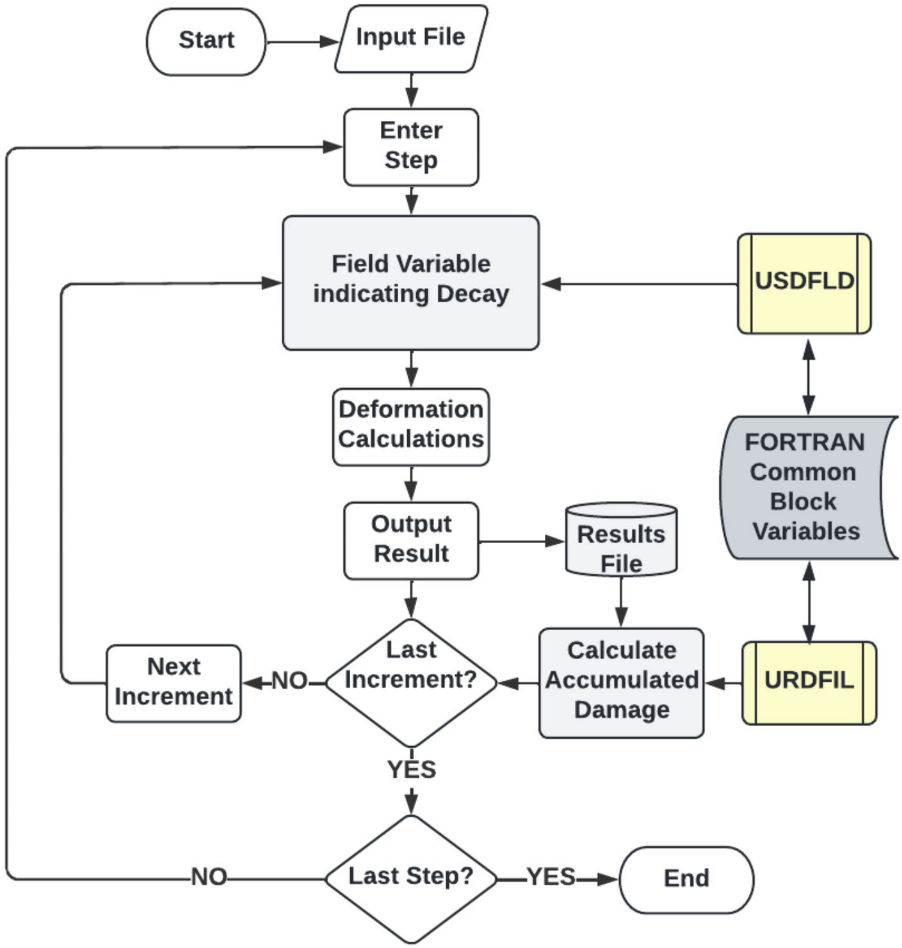

Fig. 2 Flowchart of the numerical algorithm implementing homogenised failure criterion

from the previous approach is that the computed α value is able to influence the deformation calculation results. By reducing the elastic parameters of the 'damaged' elements that exceed an α value of one, we allow higher levels of stress redistribution.

The numerical algorithm is implemented though UMAT subroutine. As shown in Fig. 3, with the initiation of bacterial decay, a 'degraded' Jacobian matrix J_d is constructed based on 50% stiffness values, which allows the stress redistribution caused by bacterial decay. At the end of each increment, a local damage accumulation coefficient α is updated. When α reaches 1, the elastic parameters (MoE and shear moduli) are further reduced to 10% of their initial values, signifying the 'failure' of the corresponding element.

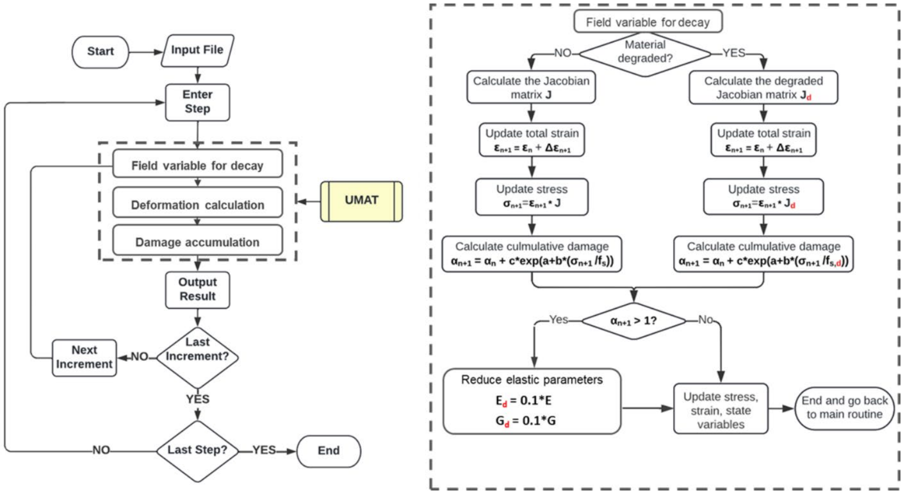

Fig. 3 Flowchart of the numerical algorithm implementing localised failure criterion

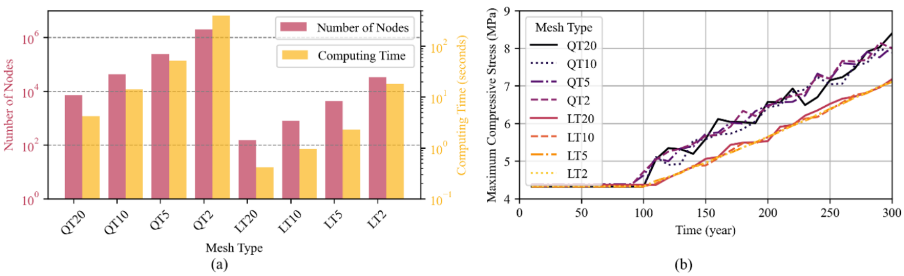

Fig. 4 Comparison of different mesh configurations: (**a**) Number of nodes and computing time, (**b**) Maximum compressive stress development in the longitudinal direction. The labels QT and LT refer to quadratic (C3D10) and linear (C3D4) tetrahedral elements, respectively. The numbers represent the mesh size in millimeters

Convergence study

Mesh sensitivity is assessed through a convergence study using the homogenized approach. The same pile problem described in Sect. 2 is modelled, except that the same decay rate of 0.2 mm/year is applied for both pile tip and pile head. Due to the round cross-section of the pile geometry, tetrahedral elements are preferred over hexahedral elements to achieve a more uniform discretization. The analysis begins with a mesh size of 20 mm, ensuring around eight elements in the diameter direction. Mesh sizes are then reduced to 10 mm, 5 mm and 2 mm, with both quadratic (C3D10) and linear (C3D4) tetrahedral elements. The total number of nodes and the computational cost for each configuration are presented in Fig. 4 (a). With the same mesh size, quadratic elements typically result in a much higher total number of nodes compared to linear elements, leading to significantly longer computation time.

To determine the optimal mesh configuration, the maximum compressive stress in the longitudinal direction is evaluated for all mesh configurations, as shown in Fig. 4 (b). Quadratic elements seem to show an earlier onset of bacterial decay compared to the linear elements. This is probably due to the higher number and thus closer spacing of integration points in C3D10 mesh configurations, which allows for earlier capture of the decay onset. Due to the progressive decay development and the subsequent stiffness reduction, the maximum stress is anticipated to increase gradually. However, mesh configurations with quadratic elements exhibit significant stress fluctuations. For linear tetrahedral elements, coarse meshes (20 mm and 10 mm) show relatively high fluctuations, whereas fine meshes (2 mm and 5 mm) produce a similar consistently increasing trend. Based on these results, the 5 mm linear tetrahedral mesh is considered to have achieved convergence. Furthermore, this configuration reduces computation time by 88% compared to the 2 mm linear tetrahedral mesh. As a result, the 5 mm linear tetrahedral mesh is considered as the optimal choice for subsequent modelling.

Results and discussion

Verification of FE model

The bacterial decay development described in sec. DOL model and bacterial decay model is compared with simulation results to verify the developed FE models. Both the homogenised approach and the localised approach yield the same results regarding decay development. The accuracy of modelling decay depth largely depends on the implemented mesh size, mesh type, and the corresponding material point locations. Some deviation from the theoretical solution is inevitable, as decay develops continuously in reality, whereas in the FE model, changes in the decay depth occur incrementally, transitioning from one material point to the adjacent one. Nevertheless, as depicted in Fig. 5, the numerical simulation captures the linear evolution well for the fast and slow decay process at the tip and head surface, respectively. The tapered decay pattern along the longitudinal direction of the pile is visualised in Fig. 6, showing good correspondence with the interpolated decay model. Moreover, the sapwood effect is also well captured, as observed from year 390, where the decay at pile tip remains within the implemented sapwood width (See Fig. 6).

Comparison of two approaches

Stress redistribution

The stress redistribution using both homogenised and localised failure criterion is illustrated for the late stage of decay development from 240 years to 270 years, shown in Fig. 7. Since the modelled problem focuses on uniaxial loading conditions, the main stress component that develops and contributes to damage accumulation is the longitudinal stress component S33. Therefore, mainly S33 is compared, which has a negative magnitude, indicating compression.

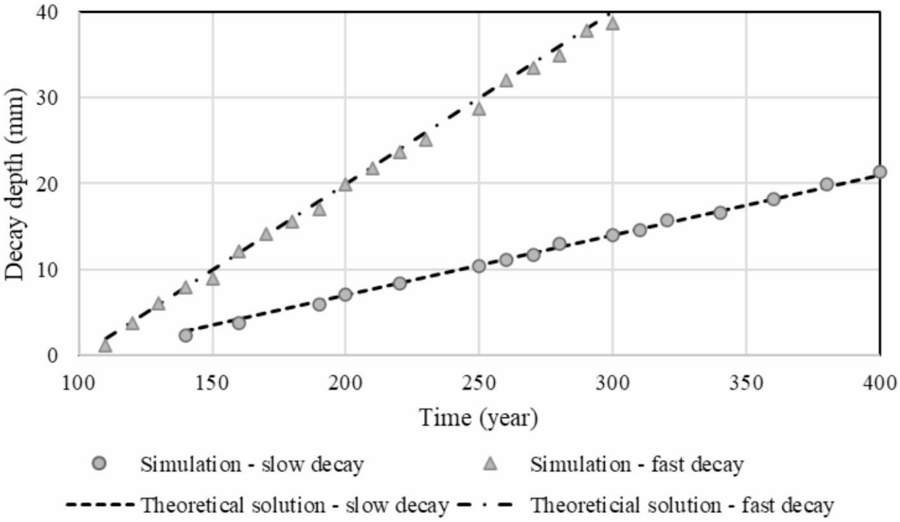

Fig. 5 Verification of bacterial decay development using both approaches

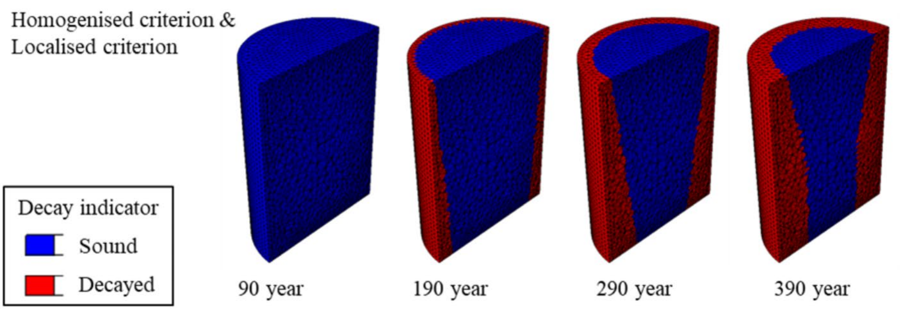

Fig. 6 The modelled bacterial decay development using both approaches (the top surface indicates pile head)

Both approaches show a much lower stress value on the outer layer that is already decayed (the decay development can be seen in Fig. 6), which can be explained by the reduced stiffness of decayed wood. As bacterial decay progresses, the overall stress value at the inner area increases, with a higher value at the pile tip (bottom surface) due to the faster decay development. Apart from that, stress concentration is observed near the boundary of inner 'sound wood', where new decay first appears. This is due to the abrupt stiffness change that we set for the simulation.

At year 240, the stress distribution using both approaches are similar. From year 250 on, a higher level of stress concentration is observed for the localised approach. This difference is a result of stress redistribution caused by stiffness reduction associated with damage accumulation.

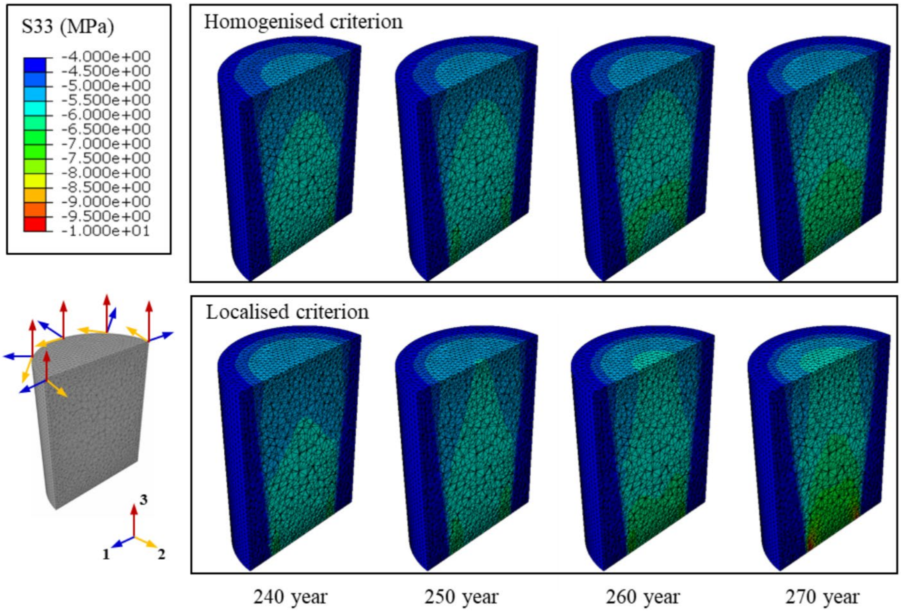

Fig. 7 Comparison of stress redistribution over time using homogenised and localised failure criterion

Damage propagation and failure

Figure 8 depicts the damage accumulation coefficient α calculated by different approaches. As the homogenised approach computes the overall damage accumulation over the whole cross section, a uniform value is calculated for all elements. An exponential increase over time is observed, corresponding to the standard DOL model of Gerhards. The structural failure is expected to be after 390 years with the implemented model.

In the localised approach, the damage accumulation coefficient α is calculated for individual elements based on the local stress level and is used as a criterion for further stiffness reduction. The increase in stress levels due to bacterial decay accelerates damage accumulation in elements near the 'sound wood' boundary. Consequently, these elements undergo an abrupt reduction in stiffness much earlier, further amplifying stress concentrations in adjacent regions. As a consequence, a large proportion of pile tip elements rapidly lose their load carrying capacity, only shortly after the first elements reach an α value of 1. At year 280, more than 20% of the entire pile elements already 'failed'.

Conclusion

Historical timber piles located below groundwater degrade over time. In this work, two mechanisms are taken into account: the cumulative damage described by duration-of-load (DOL) model, and the biological decay primarily resulting from erosion

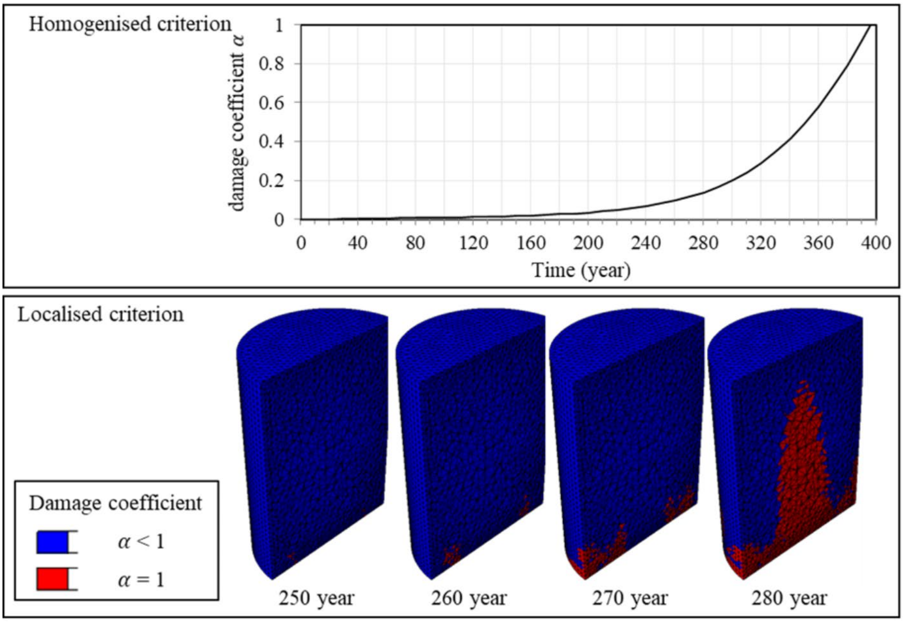

Fig. 8 Comparison of failure using homogenised and localised failure criterion

bacteria. A numerical framework is proposed based on the work by van de Kuilen and Gard (2012), which incorporates both mechanisms for the structural assessment of historical timber piles. The bacterial decay is considered as an abrupt damage process that influences the stress distribution through reduced strength and stiffness. The DOL is treated as a progressive damage process that is dependent on the stress level. By calculating the damage coefficient, failure can be determined. Herein, a homogenised failure criterion and a localised failure criterion are differentiated. The conducted case study shows that the proposed numerical framework is able to demonstrate the bacterial decay development. However, the homogenised failure criterion underestimates the effect of bacterial decay on the mechanical performance of the pile, hence predicts a much longer service life compared to the localised failure criterion.

Although this study addresses a rather simplified problem with reduced pile length, uniaxial loading, and linear decay development, the proposed numerical framework has the flexibility to be extended to more realistic loading and boundary conditions. Moreover, abrupt stiffness reduction is implemented as a preliminary attempt to account for both degradation processes. However, in reality, both processes are progressive. Further validation is needed on real historical timber piles, with a particular focus on the extent and progression of material property degradation due to bacterial decay, the decay pattern, and the strength degradation of 'undecayed wood' due to DOL effect in historical timber piles.

Acknowledgements This study was partially funded by the German Federal Ministry of Food and Agriculture through the Fachagentur Nachwachsende Rohstoffe e.V. (FNR) (grant number 22009817, HS-

Hybrid project). The authors gratefully acknowledge the support of the Bavarian State Ministry of Food, Agriculture and Forestry in the WoodVibes Project (grant number: LWF-A9-7831-26-4-1).

Author contributions C. Yang: Conceptualization, Methodology, Analysis, Writing – original draft, Writing – review & editing. A. Khaloian-Sarnaghi: Conceptualization, Methodology, Writing – review & editing, Supervision, Project administration, Funding acquisition. T. Yu: Conceptualization, Methodology, Supervision. JW. van de Kuilen: Conceptualization, Supervision, Project administration, Funding acquisition.

Funding Open Access funding enabled and organized by Projekt DEAL.

Data availability No datasets were generated or analysed during the current study.

Declarations

Competing interests The authors declare no competing interests.

References

Boutelje JB, Bravery A (1968) Observations on bacterial attack of piles supporting a Stockholm Building. J Inst Wood Sci 20:47–48

Boutelje JB, Göransson B (1975) Decay in wood constructions below the ground water table. Swed J Agric Res 5:113–12

Caulfield DF (1985) A chemical kinetics approach to the duration-of-load problem in wood. Wood Fiber Sci 17(4): 504–521

Ceccato F, Simonini P, Lionello A (2013) Long-term mechanical behavior of wooden pile foundation in Venice. 2nd International Symposium on geotechnical engineering for the preservation of monuments and historic sites. https://doi.org/10.1201/b14895

Díaz-Raviña M, Frostegård Å, Bååth E (1994) Thymidine, leucine and acetate incorporation into soil bacterial assemblages at different temperatures. FEMS (Fed. Eur Microbiol Soc) Microbiol Ecol 14(3):221–231

Elam J, Björdal C (2020) A review and case studies of factors affecting the stability of wooden foundation piles in urban environments exposed to construction work. Int Biodeterior Biodegrad 148:104913. https://doi.org/10.1016/j.ibiod.2020.104913

Gard W, Ravenshorst G, van de Kuilen J-W (2024) Historical wooden pile foundations in amsterdam: An integrated approach for the estimation of structural performance and residual service life. In Y. Endo & T. Hanazato (Eds.), Structural analysis of historical constructions, vol. 47, Springer Nature Switzerland, pp. 1370–1382. https://doi.org/10.1007/978-3-031-39603-8_110

Gerhards CC, Link CC (1987) A cumulative damage model to predict load duration characteristics of lumber. Wood a N D Fiber Sci 19

Gjelstrup Björdal C (2012) Microbial degradation of waterlogged archaeological wood. J Cult Herit 13(3):S118–S122. https://doi.org/10.1016/j.culher.2012.02.003

Grinda M (1997) Some experiences with attack of microorganisms on wooden constructions supporting foundations of houses and bridges. IRG/WP/97 10132. The International Research Group on Wood Preservation

Gunnvard P, Mattsson H, Laue J (2021) Evaluating the design criteria for light embankment piling: timber piles in road and railway foundations. Appl Sci 12(1):166. https://doi.org/10.3390/app12010166

Humar M, Balzano A, Kržišnik D, Lesar B (2021) Assessment of wooden foundation piles after 125 years of service. Forests 12(2):143. https://doi.org/10.3390/f12020143

Klaassen RKWM (2008) Bacterial decay in wooden foundation piles—Patterns and causes: A study of historical pile foundations in the Netherlands. Int Biodeterior Biodegrad 61(1):45–60. https://doi.org/10.1016/j.ibiod.2007.07.006

Laboratory FP (2021) Wood handbook—Wood as an engineering material (p. 543) [General Technical Report FPL-GTR-282.]. U.S. Department of Agriculture, Forest Service, Forest Products Laboratory

Mirra M, Pagella G, Lee M, Gard W, Ravenshorst G, Van De Kuilen J-W (2024) Characterisation of bacterial decay effects on wooden foundation piles across various historical periods. Constr Build Mater 421:135670. https://doi.org/10.1016/j.conbuildmat.2024.135670

Nielsen LF (1979) Crack failure of dead-, ramp- and combined loaded viscoelastic materials. Proceedings of First International Conference on Wood. First International Conference on Wood., Canada

Pagella G, Ravenshorst GJP (2022) Characterization of the mechanical properties of 60 timber piles retrieved from bridge 30 and 41 in Amsterdam. (TUD-M7.1-20220304-GP-v3)

Pagella G, Mirra M, Ravenshorst G, Gard W, Van De Kuilen J-W (2024) Characterization of the remaining material and mechanical properties of historic wooden foundation piles in Amsterdam. Constr Build Mater 450:138616. https://doi.org/10.1016/j.conbuildmat.2024.138616

Przewłócki I, Dardzińska I, Świniański J (2005) Review of historical buildings' foundations. Géotechnique 55(5):363–372. https://doi.org/10.1680/geot.2005.55.5.363

Rehbein M, Koch G, Schmitt U, Huckfeldt T (2013) Topochemical and transmission electron microscopic studies of bacterial decay in pine (Pinus sylvestris L.) harbour foundation piles. Micron (Oxford England: 1993) 44:150–158

Sundararaj R (ed) (2022) Science of wood degradation and its protection. Springer Singapore. https://doi.org/10.1007/978-981-16-8797-6

Svensson S (2009) Duration of load effects of solid wood: A review of methods and models. Wood Mater Sci Eng 4(3–4):115–124. https://doi.org/10.1080/17480270903326157

Van de Kuilen JW, Gard W (2012) Residual service life Estimation using damage accumulation models. World Conference on Timber Engineering 2012, Auckland

Van de Kuilen JWG, Beketova-Hummel O, Pagella G, Ravenshorst GJP, Gard WF (2022) An integral approach for the assessment of timber pile foundations. World Conference on Timber Engineering 2021, Santiago, Chile

Van der Put TACM (1989) Deformation and damage processes in wood. Delft University

Wood LW (1951) Relation of strength of wood to duration of load

Zelada-Tumialan GA, Konicki W, Westover P, Vatovec M (2013) Untreated submerged timber pile foundations: part 1: understanding biodegradation and compressive strength. Struct Mag December 2013: 9–11

Zelada-Tumialan GA, Konicki W, Westover P, Vatovec M (2014) Untreated submerged timber pile foundations: part 2: estimating remaining service life. Struct Mag January 2014: 10–13